Bioactive Materials 5 (2020) 185–191

Contents lists available at ScienceDirect

Bioactive Materials

journal homepage: http://www.keaipublishing.com/biomat

Polycaprolactone/polysaccharide functional composites for low-temperature fused deposition modelling

Yu-Qing Zhao, Ji-Hao Yang, Xiaokang Ding, Xuejia Ding, Shun Duan*, Fu-Jian Xu**

State Key Laboratory of Chemical Resource Engineering, Key Lab of Biomedical Materials of Natural Macromolecules (Beijing University of Chemical Technology), Ministry of Education, Beijing Laboratory of Biomedical Materials, Beijing University of Chemical Technology, Beijing, 100029, China

ARTICLE INFO

Keywords:
Fused deposition modelling
Melt blending
Polycaprolactone
Composite
Antibacterial

ABSTRACT

Fused deposition modelling (FDM) is a commonly used 3D printing technology. The development of FDM materials was essential for the product quality of FDM. In this work, a series of polycaprolactone (PCL)-based composites for low-temperature FDM were developed. By melt blending technique, different ratios of starch were added into PCL to improve the performances of FDM, and the printability, tensile strength, rheological properties, crystallization behaviors and biological performances of the composites were studied. The PCL/starch composite had the best performance in FDM process with the starch ratio of 9 ph at 80–90 °C. The melting strength and solidification rate of PCL/starch composites were improved. The starch also increased the crystallization temperature, degree of crystallinity and crystallization rate of PCL/starch composites, while had no negative effects on the tensile strength of PCL. Due to the low printing temperature, various kinds of bioactive components were added into PCL/starch composites for preparation of antibacterial and biocompatible materials for FDM. The present work provides a new method to develop novel low-temperature FDM materials with various functions.

1. Introduction

Three-dimensional (3D) printing is an advanced technology for customized manufacturing [1–3]. By stacking materials layer by layer, objects could be produced based on computer-aided design models by 3D printing, which has been widely applied in medical field [4,5], part manufacturing [6], automobile industry [7], and so on. The 3D printing technology has various types, including fused deposition modelling (FDM) [8], stereo lithography appearance (SLA) [9], selective laser sintering (SLS) [10], laminated object manufacturing (LOM) [11], patternless casting manufacturing (PCM) [12], and so on. Among all the types of 3D printing, FDM is commonly used because of its low the cost and easy operation [13,14]. In the FDM process, the material has the very significant influence on the quality and function of the printed products [15–17]. Therefore, it has high theoretic meaning and realistic value to develop high-performance materials for FDM.

The common-used thermoplastic materials for FDM, such as polylactic acid [18], poly(acrylonitrile-*co*-butadiene-*co*-styrene) [19] and polycarbonate [20], were manufactured at the temperature higher than 200 °C. The high manufacturing temperature leads to high energy consumption and low safety, especially for small-scale household FDM printer. Moreover, it was reported that volatile organic compounds (VOC) and air-borne micro-particles of plastics were produced continuously during the FDM processes under high temperature, which will be harmful to the health of the users [21,22]. Moreover, the high manufacturing temperature hinders the addition of bioactive components into the FDM materials, limiting the functionalization of these materials.

Polycaprolactone (PCL) is a kind of linear aliphatic polyester with good flexibility, machinability, biodegradability and biocompatibility, which is semi-crystalline under room temperature, and the melting temperature of PCL ranges from 59 to 64 °C. The above-mentioned properties makes PCL a potential candidate of functional FDM materials [23]. However, pristine PCL possesses many disadvantages for FDM, including low solidifying rate and insufficient melt strength, which are obstacles of large-scale application apply of PCL as a FDM material [24,25]. Recently, many types of PCL-based 3D printing materials were developed [26,27], but the raw materials of these materials were mainly slurry and the manufacturing process needed dedicated devices for modelling.

Peer review under responsibility of KeAi Communications Co., Ltd.
* Corresponding author.
** Corresponding author.
E-mail addresses: duanshun@mail.buct.edu.cn (S. Duan), xufj@mail.buct.edu.cn (F.-J. Xu).

https://doi.org/10.1016/j.bioactmat.2020.02.006
Received 29 August 2019; Received in revised form 2 January 2020; Accepted 5 February 2020

In this work, we developed a series of functional PCL/starch composites for low-temperature FDM by melt blending technique. Different ratios of starch were blended with PCL to prepare PCL/starch composites for FDM. The 3D-printability, tensile strength, rheological properties, crystallization behaviors and biological performances of the composites were studied. This work provides a novel method to develop functional materials for low-temperature FDM.

2. Experimental section

2.1. Materials

PCL (Perstorp 6800) was purchased from Solvay, USA. Soluble starch was purchased from Sigma-Aldrich, USA. Corn starch (M_w = 14.4 × 10^3 kDa) and potato starch (M_w = 25.2 × 10^3 kDa) were purchased from Aladdin, China. Quaternary ammonium-73 was purchased from Tianjin Ringpu Biotechnology Co., Ltd., China. Polyhexamethylene biguanidine (PHMB) was purchased from Guangdong AONA New Materials Co. Ltd., China. Nano-hydroxyapatite (nHA, with the length of ~100 nm and diameter of 20 nm) was purchased from Beijing DK Nano Technology Co. Ltd., China.

2.2. Preparation of PCL/starch composites

PCL, soluble starch, corn starch and potato starch were placed in an air-blower-driver dryer at 50 °C for 2 h. After drying, 100 g of PCL was respectively mixed with 1 g, 3 g, 5 g, 7 g, 9 g and 11 g of each kind of starch. The mixtures were thoroughly blended with a high-speed mixer and then extruded by a twin-screw extruder. The parameters of the twin-screw extruder were shown as Table 1. After being pelletized, the composites were dried completely.

2.3. Preparation of antibacterial PCL/starch composites

The PCL/starch composite, quaternary ammonium-73 and PHMB were placed in an air-blower-driver dryer at 50 °C for 2 h. After drying, 0.01 g, 0.1 g and 1 g of quaternary ammonium-73 were respectively mixed with 100 g of dried PCL/starch composite, and then treated with high-speed mixer. The mixtures were extruded by a twin-screw extruder with the parameters shown in Table 1. Similarly, 0.1 g, 1 g and 10 g of PHMB were also mixed with PCL/starch composite as described above. The prepared antibacterial composites were pelletized and dried completely.

2.4. Preparation of nHA-modified PCL/starch composites

The PCL/starch composite and nHA were placed in an air-blower-driver dryer at 50 °C for 2 h. After drying, 10 g of nHA was mixed with 100 g of dried PCL/starch composite, and then treated with high-speed mixer. The mixtures were extruded by a twin-screw extruder with the parameters shown in Table 1. Finally, the samples were pelletized and dried completely.

2.5. Preparation of filaments for 3D printing

The filaments of each kind of composite were prepared by a single-screw extruder, and the parameters of preparation were shown in Table 1. The diameter of the filaments was confined as 1.75 ± 0.05 mm by controlling the rotating speed of tractor. The prepared filaments were collected on take-up reels by a rotary thread rolling machine.

Table 2
Parameter setting of FDM printer.

Nozzle temperature	Plate Temperature	Printing resolution	Printing speed	Feeding speed	Filling ratio
90 °C	25 °C	0.2 mm	40 mm/s	90 mm/s	100%

2.6. Characterization

The 3D-printing performances were evaluated by a FDM printer (Replicator X2, Makerbot, USA). The filament samples were used to prepare a cubic modal with the size of 20 mm × 20 mm × 10 mm. The parameters of FDM printer were shown in Table 2. ABS resin was taken as a reference.

The tensile strength was measured by a universal testing machine (UTM-1422, Jinjian, China). The pellet samples were dried at 50 °C for 2 h and then prepared into thin sheets with the thickness of 1 mm via hot-press by a plate vulcanizing machine. After cooling, the sheets were cut into standard dumbbell-shaped samples with the effective length of 25 mm and effective width of 4 mm. The testing of tensile strength was performed at the stretching speed of 100 mm/min following GB/T 1040–2006, and five duplicate samples were tested in each group.

The rheological properties were characterized by rheometer (HR-1, Waters, USA). The samples for rheological testing were prepared by a plate vulcanizing machine and cut into round slices with the diameter of 25 mm and the thickness of 1 mm. For dynamic frequency scanning, the temperature was set as 90 °C, while the strain was 5% and angular velocity (ω) was 0.5–100 rad/s. For viscosity-temperature curve, the temperature was set as 60–90 °C with the heating rate of 3 °C/min, and the strain rate was 1/s.

The crystallization behaviors were studied by a differential scanning calorimetry (DSC, Q20, TA Instruments, USA) in nitrogen atmosphere. For isothermal crystallization, the samples were heated to 100 °C with the heating rate of 10 °C/min and kept for 3 min to eliminate the heat history. Then, the samples were cooled to 40 °C at the cooling rate of 100 °C/min and kept for 20 min. For non-isothermal crystallization, the samples were heated to 100 °C with the heating rate of 10 °C/min and kept for 3 min to eliminate the heat history. Subsequently, the samples were cooled from 100 °C to 0 °C and then heated from 0 °C to 100 °C.

For polarizing microscope (POM) observation, a pellet of each sample were placed onto a glass slide and heated to 90 °C by a heating stage. Then, the heated sample was pressed by another glass slide into a thin sheet. The sample along with the heating stage were moved to POM. The initial temperature was set as 75 °C, and then cooled to 47 °C with the cooling rate of 2 °C/min. The crystallization process was observed by a 10 × objective lens.

2.7. Antibacterial test

For inhibition zone test, the samples with quaternary ammonium-73 and PHMB were cut into round slices with the diameter of 5 mm and sterilized by 75% ethanol. *S. aureus* was chosen as the representative pathogen. In a six-well culture plate, the solid lysogeny broth (LB) media were placed. In each well, 0.5 mL of *S. aureus* suspension with

Table 1
Extruder parameter setting.

	Zone 1/°C	Zone 2/°C	Zone 3/°C	Zone 4/°C	Screw speed/(mm/s)
Twin-screw extruder	50	70	90	70	20
Single-screw extruder	80	–	–	75	30

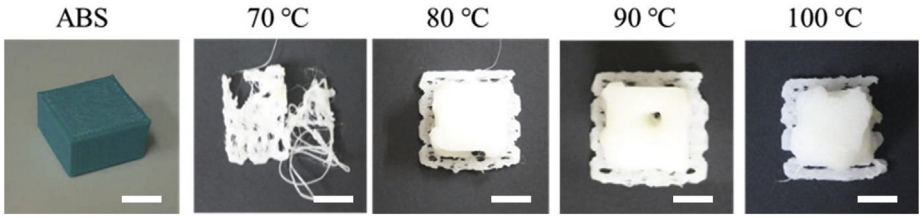

Fig. 1. General views of 3D-printed ABS and pristine PCL samples at different temperature (scale bar = 1 cm).

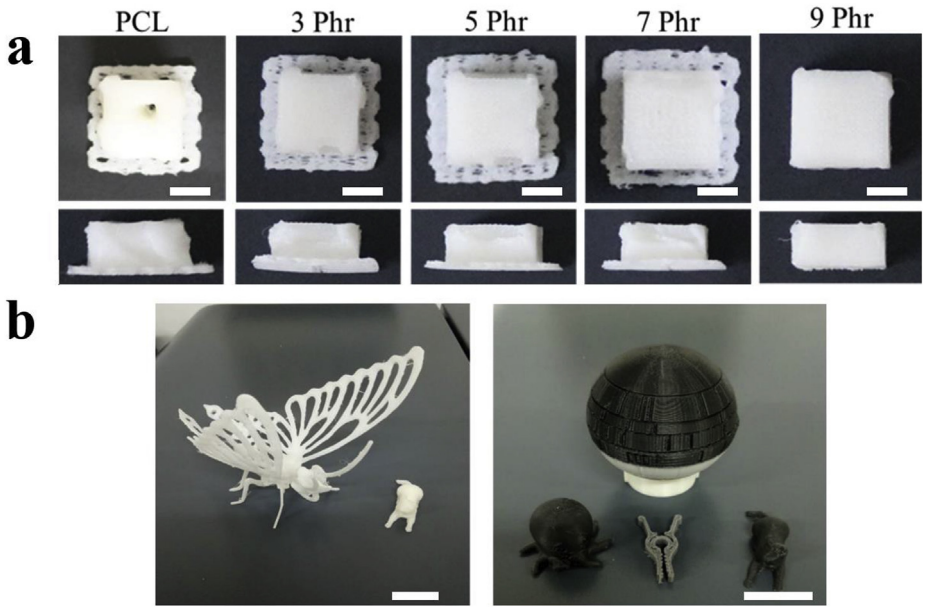

Fig. 2. (a) Representative images of 3D-printed PCL/starch composites with various ratios of starch (scale bar = 1 cm); (b) FDM products prepared by PCL composite with 9 phr of starch (scale bar = 2 cm).

Table 3
Completeness of 3D-printed PCL/starch composites.

Starch ratio/phr	PCL	1	3	5	7	9
C	83.3	94.3	95.9	96.8	97.5	99.0

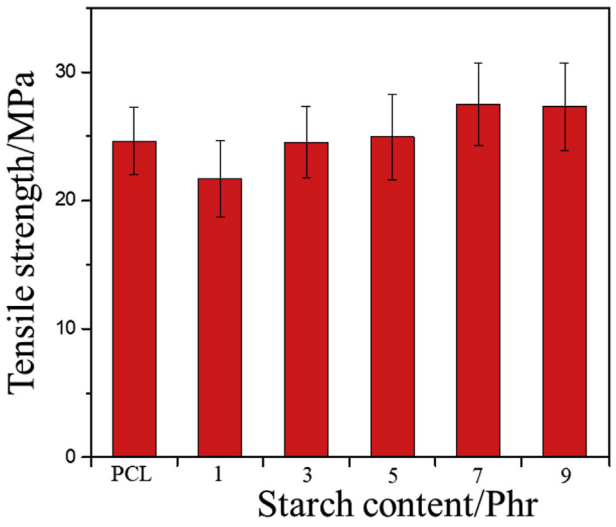

Fig. 3. Tensile strengths of PCL/starch composites at the additive ratios for 1–9 phr.

the bacterial density of 10^5 CFU/mL was inoculated and spread. Then the samples were placed into the center of each well, and the culture plates were incubated for 24 h at 37 °C. After incubation, the inhibition zones were observed.

Based on QB/T 2591-2003, *E. coli* and *S. aureus* were used for film sticking test. The samples were cut into sheets with the size of 20 mm × 20 mm and placed into culture dishes. On each sample, 32 μL of bacterial suspension with the density of 10^5 CFU/mL was inoculated, and then a glass slice with the same size was covered on the sample. The samples were incubated for 24 h at 37 °C. After incubation, the samples and the glass slice were thoroughly rinsed by 5 mL of normal saline. Then, 20 μL of the rinsed solution was moved onto solid LB culture media and cultured for 24 h at 37 °C. After incubation, the bacterial colonies on the culture media were observed and counted.

2.8. In vitro cytotoxicity test

A fibroblast cell line, L929, was taken for in vitro cytotoxicity test. In a 96-well culture plate, 5×10^3 cells were seeded into each well and incubated for 24 h at 37 °C under 5% of CO_2. Following ISO 10993-2009, the sterilized samples with nHA were soaked in DMEM media supplemented with 10% fetal bovine serum, 100 U/mL of penicillin and 100 mg/mL of streptomycin for 24 h at 37 °C to prepare extracts. After 24 h incubation, the culture media were removed. The extracts were added into the wells and cultured for another 24 h. The fresh culture medium was taken as a control group. After culture, the cell viabilities were evaluated by CCK-8 method [28]. The OD values of CCK-8 were determined at the wavelength of 450 nm by a microplate reader (Bio-rad 680, USA). The relative cell viability of control group was defined as 100%.

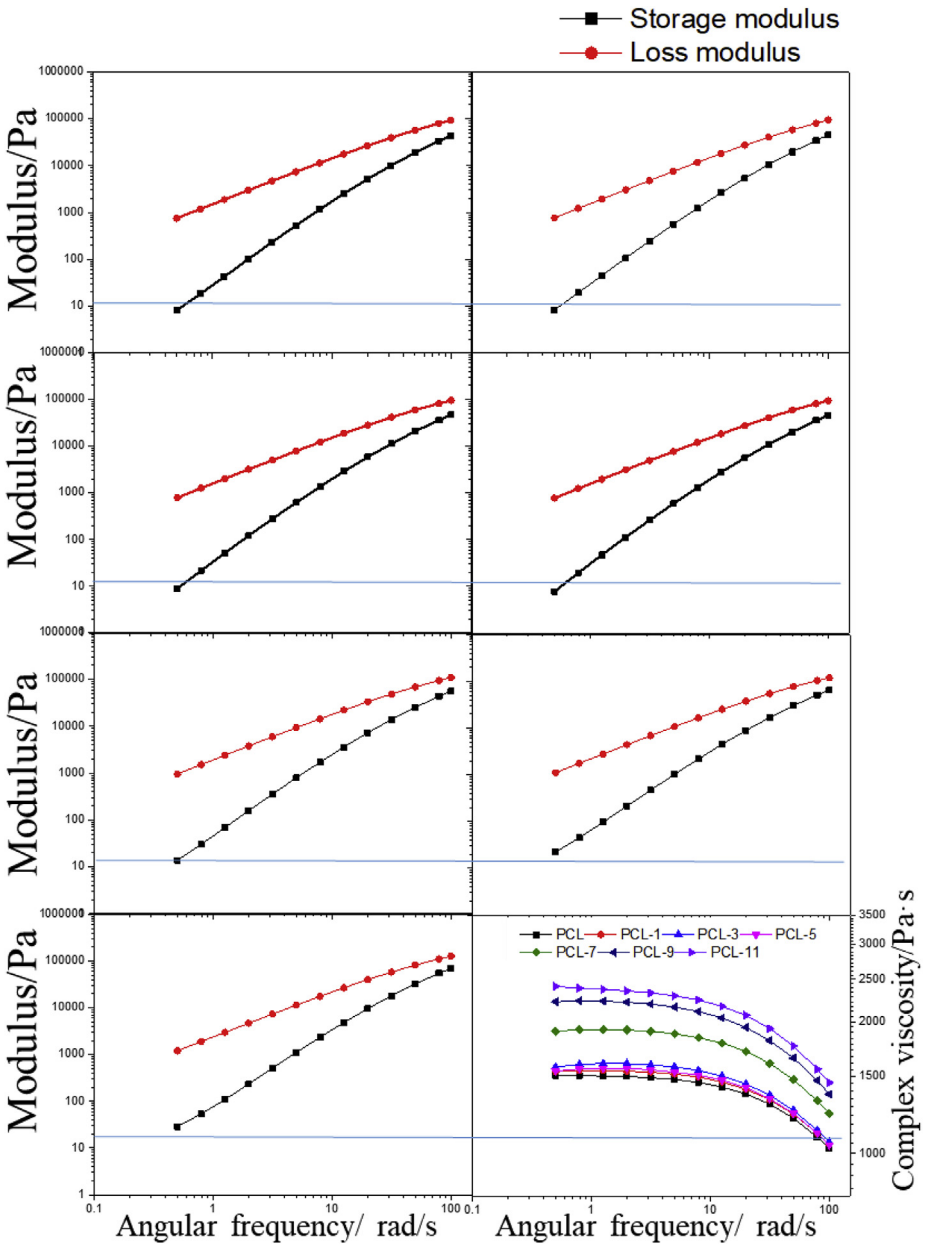

Fig. 4. Storage modulus, loss modulus and complex viscosity of PCL/starch composites at the additive ratios for 1–11 phr by frequency scanning.

2.9. Statistical analysis

At least three samples were tested in each time point. The results were reported as mean ± standard deviation (SD). When two groups were compared, the differences were assessed by the paired *t*-test. A significance level of $p = 0.05$ were performed using Origin 8.1 software.

3. Results and discussion

3.1. 3D printing performances

To determine the temperature range of FDM process of PCL, cubic models were first printed by pristine PCL at 70 °C, 80 °C, 90 °C and 100 °C. As shown in Fig. 1, the integrity of the printed PCL models at 80 °C and 90 °C was higher than that at 70 °C and 100 °C. When the printing temperature was lower than 80 °C, the fluidity of melt PCL was low, which was difficult to pass through the nozzle. At the printing temperature higher than 90 °C, the melt strength solidification rate of PCL decreased, leading to collapse of the printed model. Therefore, the printing temperature was determined between 80 °C and 90 °C. However, the quality of 3D-printed pristine PCL models was still lower than that of ABS.

Due to the appropriate cost, particle diameter, thermostability and nucleation promoting property, starch was chosen as the additive. In order to improve the quality of 3D-printed PCL products, starch was used to prepare PCL/starch composite. To optimize the ratio of starch, different amounts of starch (3 phr, 5 phr, 7 phr, 9 phr and 11 phr) were added into PCL. For quantitative evaluation of the qualities of 3D-printed models, we introduced an index of completeness (C),

$$C = V^*/V \times 100$$

where V^* was the defected volume and V was the total volume of the preset model. After addition of starch, the qualities of 3D-printed models were improved (Fig. 2a). Furthermore, the quality of the printed products increased with from 3 phr to 9 phr (Table 3). The completeness of printed model reached 99 with the starch ratio of 9 phr. When

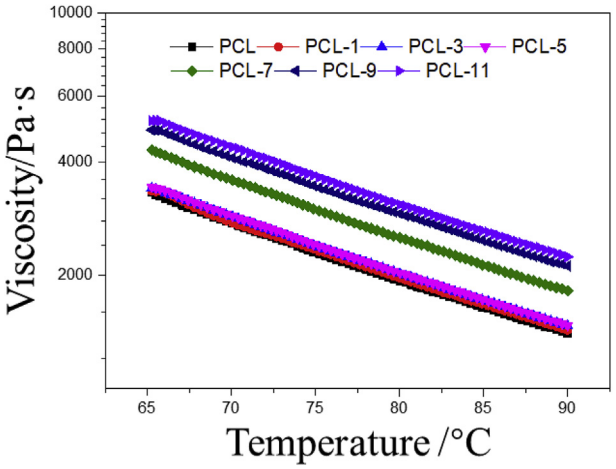

Fig. 5. Viscosity-temperature curves of PCL/starch composites at the additive ratios for 1–11 phr.

11 phr of starch was added, the viscosity of the melt composite was too high and blocked the nozzle. Therefore, 9 phr was the optimal ratio of starch for 3D printing of PCL. The composite with 9 phr of starch had good performance in FDM process, which could be precisely manufactured into complicated constructions (Fig. 2b).

3.2. Mechanical property

When the filaments were applied in the FDM 3D printer, they were pulled by a tractor. Therefore, the tensile strength was essential for FDM materials. To evaluate the effects of starch on the mechanical property of PCL/starch composite, the tensile strength was studied. As shown in Fig. 3, the starch had no negative effects on the tensile strength of the composites, indicating the good compatibility between starch and PCL matrix. When the adding ratio was 7 and 9, the strength of PCL/starch composites showed slight increasing, which might due to the higher degree of crystallinity induced by starch [29]. The result of tensile strength demonstrated the good mechanical property of PCL/starch composites.

3.3. Rheological behaviors

The printable properties of the PCL/starch composites were evaluated by rheological behaviors. When the samples were printed by a FDM 3D printer, the printing speed (v) was 40 mm/s (Table 2). The radius (r) of the round sample for rheological test was 12.5 mm, therefore, the angular frequency (ω) was determined as 4.5 rad/s by the formula $\omega = \frac{3v}{2r}$. Under this angular frequency, the printability was assessed by the storage modulus (G') and loss modulus (G''). As shown in Fig. 4, the G'' of the samples was higher than G', which indicated the strong interlayer adhesive force. While starch was added, both G' and G'' increased with the amount of starch, which might due to that the melt strength of the composite was improved by starch [30]. Therefore, the printability of PCL/starch composites was improved due to the enhanced melt strengths. Based on the results of dynamic frequency scanning, the complex viscosities (η^*) of the samples increased with the adding amounts of starch. When the adding amounts were less than 7 phr, the increasing levels of η^* were relatively low, because the adding amounts were small and had little effects on η^* of the composites. At the adding amounts of 7 phr and 9 phr, the effects of starch on η^* of the composites were significant. While starch was added more than 9 phr, the increasing of η^* slowed down. Moreover, the viscosity-temperature curves (Fig. 5) also demonstrated the viscosifying effects of starch on melt PCL composites. These rheological results indicated that the PCL/starch composites with adding ratios of 7 phr and 9 phr could be printed at 80–90 °C.

3.4. Thermal and crystallization properties

The crystallization temperature, degree of crystallinity and crystallization rate were studied by DSC. The isothermal crystallization properties were shown in Fig. 6a. After the addition of starch, the crystallization rates increased, which leaded to complete crystallization in a short time. The results of non-isothermal crystallization (Fig. 6b and Table 4) indicated that starch could raise the crystallization temperature of PCL composites. The high crystallization temperature increased the solidification rate of melt PCL composites, which was beneficial for FDM process.

The crystallization process was observed by POM (Fig. 7). The POM images illustrated that starch could increase the crystallization rate of PCL composites. Along with the increasing of starch ratios, the crystallization rate also increased, which was consistent with the DSC results. In addition, the POM images also showed that the crystal cores appeared around the starch particles, which demonstrated that starch played the role of nucleation promoter during the crystallization process of PCL/starch composites.

3.5. Antibacterial performances and biocompatibility

Compared with the traditional FDM materials, such as PLA and ABS, PCL/starch composites could be printed under relative low temperature (80–90 °C). Therefore, various kinds of organic components, which would decompose under high temperature, could be added into the composites for functionalization. For antibacterial functionalization, two kinds of organic antibacterial agents, quaternary ammonium-73 and PHMB, were added (Fig. 8a). When the ratios of quaternary ammonium-73 and PHMB were 0.1 phr and 1 phr, respectively, the composites possessed high antibacterial efficiency (Fig. 8b). The diameters

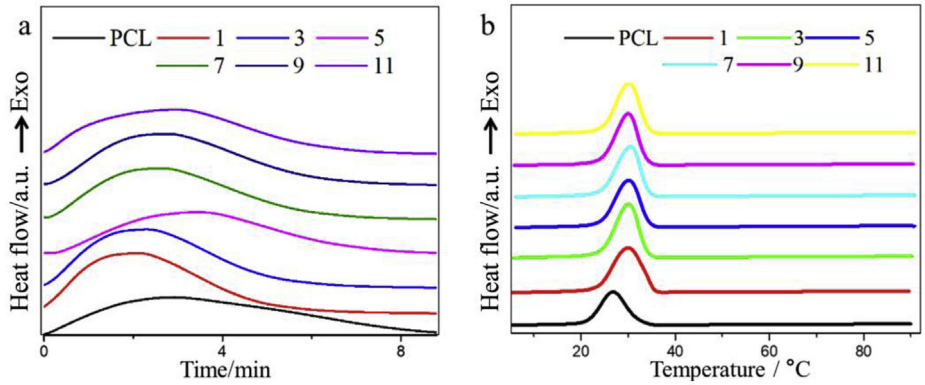

Fig. 6. Crystalline curves of PCL/starch composites at the additive ratios for 1–11 phr: (a) isothermal crystallization; (b) non-isothermal crystallization.

Table 4
DSC data of non-isothermal crystallization of PCL/starch composites.

Starch ratio (phr)	0	1	3	5	7	9	11
T_o/°C	26.76	30.18	29.59	29.06	29.43	33.20	29.10
T_c/°C	32.17	35.74	33.51	33.34	33.20	33.06	33.20
θ/%	100.0	150.2	147.7	133.2	142.0	137.2	139.6

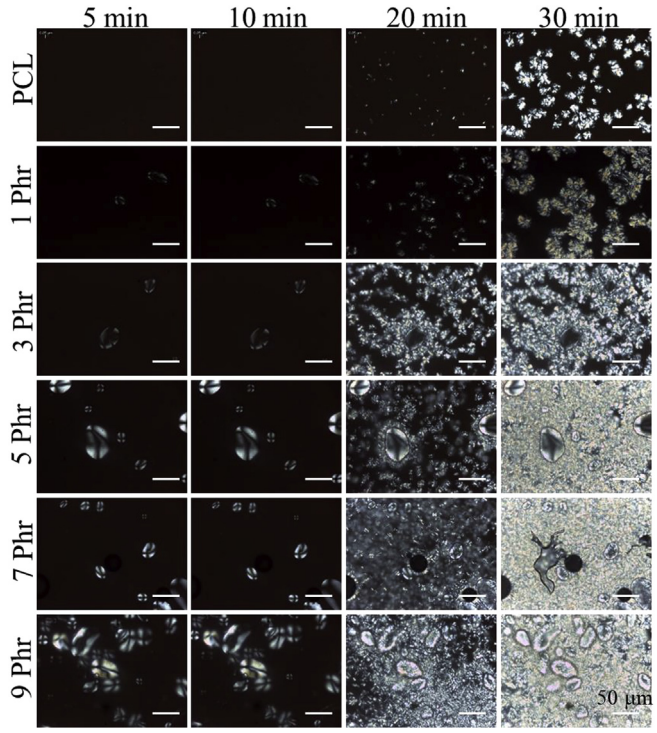

Fig. 7. Crystallization process of PCL/starch composites at the additive ratios for 1–11 phr by representative POM images.

of the inhibition zones increased with the adding ratio of the antibacterial agents. Furthermore, the antibacterial performances were also evaluated by film sticking test to simulate direct contacting (Fig. 9). For *S. aureus* and *E. coli*, the samples showed good antibacterial efficiencies, which was coincident with the results of inhibition zones. When the additive ratio of quaternary ammonium-73 was 0.05 phr, the antibacterial ratios were higher than 99.99% against *S. aureus* and 90% against *E. coli*, respectively. For PHMB, the antibacterial ratios were higher than 99.99% against both *S. aureus* and *E. coli* when the additive ratio was higher than 1 phr. These results indicated that the organic antibacterial agents were not affected by the low temperature in FDM process of PCL/starch composites. Therefore, antibacterial FDM materials could be prepared by direct addition of organic antibacterial agents into the PCL/starch composites.

Moreover, PCL is a biodegradable polyester, which could be used in bone tissue engineering [31]. The nHA was also added to improve the osteogenic activity of the composites [32]. Because the additive ratio of nHA was low, it did not affect the processability. Biocompatibility is an essential property for PCL/starch composites as tissue engineering materials. As a preliminary study, the cytotoxicity of PCL/starch composites was evaluated. As shown in Fig. 10, the PCL/starch (PCL/ST) composite and PCL/starch with nHA (PCL/ST/HA) had no toxicity to cells. Therefore, the low-cytotoxic PCL/ST/HA composites might be used as FDM materials for the personalized therapy of bone defects.

4. Conclusion

In summary, a series of PCL starch composites for low-temperature FDM 3D printing were developed and further functionalized. By blending modification, the qualities of 3D-printed products were improved. When the ratio of starch was 9 phr, the PCL/starch composite had the best performance in FDM process. The addition of starch enhanced the melting strength and solidification rate of PCL/starch composites. The starch increased the crystallization temperature, degree of crystallinity and crystallization rate of PCL/starch composites, which was beneficial for FDM process. The starch components also had no negative effects on the mechanical properties of PCL. Based on the low printing temperature, various kinds of bioactive components were added into PCL/starch composites for preparation of antibacterial and biocompatible materials for FDM, providing additional functions for FDM materials.

CRediT authorship contribution statement

Yu-Qing Zhao: Data curation, Formal analysis, Writing - original draft. **Ji-Hao Yang:** Methodology. **Xiaokang Ding:** Validation. **Xuejia Ding:** Validation. **Shun Duan:** Conceptualization, Writing - review & editing. **Fu-Jian Xu:** Project administration.

Declaration of competing interest

The authors declare no conflict of interest.

Acknowledgements

This work was supported by National Natural Science Foundation of China (Grant No. 51873012), National Key Research and Development Program of China (Grant No. 2016YFC1100404), Beijing Municipal Natural Science Foundation (Grant No. 7161001), Fundamental

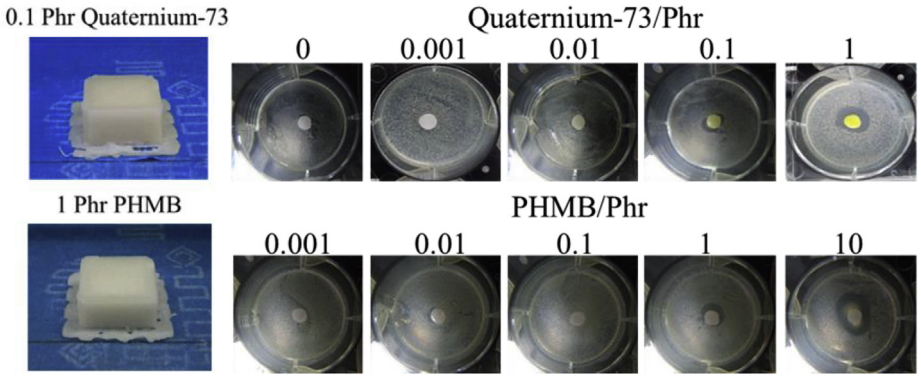

Fig. 8. (a) Images of antibacterial PCL/starch composite samples manufactured by FDM; (b) inhibition zones of antibacterial PCL/starch composites with different contents of quaternary ammoniym-73 and PHMB.

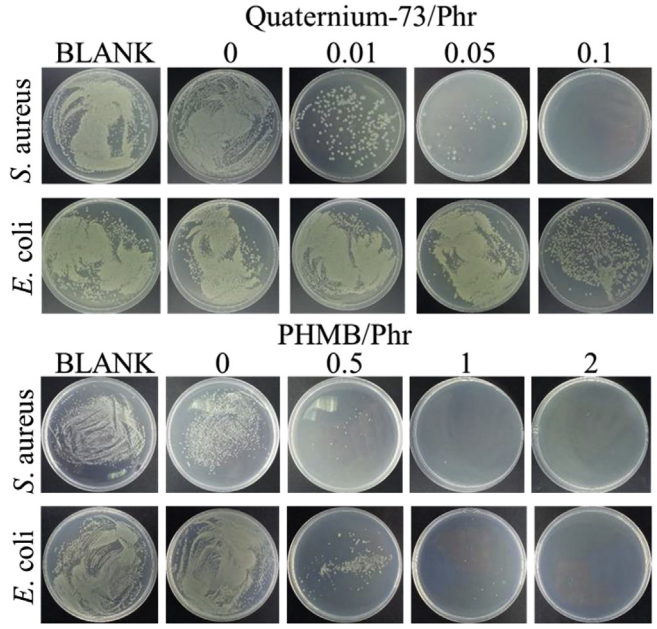

Fig. 9. Bacterial colonies of antibacterial PCL/starch composites with different contents of quaternary ammoniym-73 and PHMB by film sticking test.

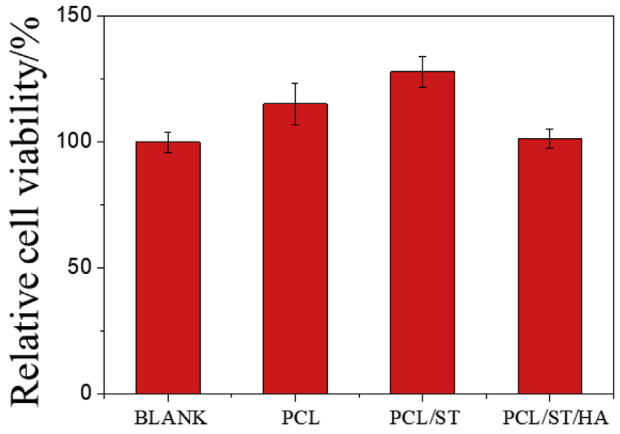

Fig. 10. Cytotoxicity of PCL, PCL/ST and PCL/ST/HA composites represented by relative cell viability. Blank groups was defined as 100%.

Research Funds for the Central Universities (Grant No. XK1802-2) and Research Projects on Biomedical Transformation of China-Japan Friendship Hospital (Grant No. PYBZ1832).

References

[1] T. DebRoy, H.L. Wei, J.S. Zuback, T. Mukherjee, J.W. Elmer, J.O. Milewski, A.M. Beese, A. Wilson-Heid, A. De, W. Zhang, Additive manufacturing of metallic components - process, structure and properties, Prog. Mater. Sci. 92 (2018) 112–224.
[2] T.D. Ngo, A. Kashani, G. Imbalzano, K.T.Q. Nguyen, D. Hui, Additive manufacturing (3D printing): a review of materials, methods, applications and challenges, Compos. Pt. B 143 (2018) 172–196.
[3] S. Bose, D.X. Ke, H. Sahasrabudhe, A. Bandyopadhyay, Additive manufacturing of biomaterials, Prog. Mater. Sci. 93 (2018) 45–111.
[4] S.H. Lim, H. Kathuria, J.J.Y. Tan, L.F. Kang, 3d printed drug delivery and testing systems - a passing fad or the future? Adv. Drug Deliv. Rev. 132 (2018) 139–168.
[5] G. Turnbull, J. Clarke, F. Picard, P. Riches, L. Jia, F. Han, B. Li, W. Shu, 3d bioactive composite scaffolds for bone tissue engineering, Bioact. Mater. 3 (2018) 278–314.
[6] J.M. Chacon, M.A. Caminero, P.J. Nunez, E. Garcia-Plaza, I. Garcia-Moreno, J.M. Reverte, Additive manufacturing of continuous fibre reinforced thermoplastic composites using fused deposition modelling: effect of process parameters on mechanical properties, Compos. Sci. Technol. 181 (2019) 107688.
[7] I.F. Ituarte, S. Chekurov, J. Tuomi, J.E. Mascolo, A. Zanella, P. Springer, J. Partanen, Digital manufacturing applicability of a laser sintered component for automotive industry: a case study, Rapid Prototyp. J. 24 (2018) 1203–1211.
[8] N. Mohan, P. Senthil, S. Vinodh, N. Jayanth, A review on composite materials and process parameters optimisation for the fused deposition modelling process, Virtual Phys. Prototyp. 12 (2017) 47–59.
[9] Y. Zou, Q. Han, X.S. Weng, Y.W. Zou, Y.Y. Yang, K.S. Zhang, K.R. Yang, X.L. Xu, C.Y. Wang, Y.G. Qin, J.C. Wang, The precision and reliability evaluation of 3-dimensional printed damaged bone and prosthesis models by stereo lithography appearance, Medicine 97 (2018) e9797.
[10] L.C. Zhang, Y.J. Liu, S.J. Li, Y.L. Hao, Additive manufacturing of titanium alloys by electron beam melting: a review, Adv. Eng. Mater. 20 (2018) 1700842.
[11] G. Zhang, H. Chen, S.B. Yang, Y.Z. Guo, N. Li, H.W. Zhou, Y. Cao, Frozen slurry-based laminated object manufacturing to fabricate porous ceramic with oriented lamellar structure, J. Eur. Ceram. Soc. 38 (2018) 4014–4019.
[12] C.J. Bae, D. Kim, J.W. Halloran, Mechanical and kinetic studies on the refractory fused silica of integrally cored ceramic mold fabricated by additive manufacturing, J. Eur. Ceram. Soc. 39 (2019) 618–623.
[13] K. Rane, M. Strano, A comprehensive review of extrusion-based additive manufacturing processes for rapid production of metallic and ceramic parts, Adv. Manuf. 7 (2019) 155–173.
[14] D. Pranzo, P. Larizza, D. Filippini, G. Percoco, Extrusion-based 3d printing of microfluidic devices for chemical and biomedical applications: a topical review, Micromachines 9 (2018) 374.
[15] S.C. Ligon, R. Liska, J. Stampfl, M. Gurr, R. Mulhaupt, Polymers for 3d printing and customized additive manufacturing, Chem. Rev. 117 (2017) 10212–10290.
[16] B. Brenken, E. Barocio, A. Favaloro, V. Kunc, R.B. Pipes, Fused filament fabrication of fiber-reinforced polymers: a review, Addit. Manuf. 21 (2018) 1–16.
[17] H. Klippstein, A.D.D. Sanchez, H. Hassanin, Y. Zweiri, L. Seneviratne, Fused deposition modeling for unmanned aerial vehicles (UAVS): a review, Adv. Eng. Mater. 20 (2018) 1700552.
[18] W.-F. Yang, L. Long, R. Wang, D. Chen, S. Duan, F.-J. Xu, Surface-modified hydroxyapatite nanoparticle-reinforced polylactides for three-dimensional printed bone tissue engineering scaffolds, J. Biomed. Nanotechnol. 14 (2018) 294–303.
[19] H. Amiruddin, M.F. Bin Abdollah, N.A. Norashid, Comparative study of the tribological behaviour of 3d-printed and moulded abs under lubricated condition, Mater. Res. Express 6 (2019) 085328.
[20] J.M. Puigoriol-Forcada, A. Alsina, A.G. Salazar-Martin, G. Gomez-Gras, M.A. Perez, Flexural fatigue properties of polycarbonate fused-deposition modelling specimens, Mater. Des. 155 (2018) 414–421.
[21] P. Byrley, B.J. George, W.K. Boyes, K. Rogers, Particle emissions from fused deposition modeling 3d printers: evaluation and meta-analysis, Sci. Total Environ. 655 (2019) 395–407.
[22] P. Azimi, D. Zhao, C. Pouzet, N.E. Crain, B. Stephens, Emissions of ultrafine particles and volatile organic compounds from commercially available desktop three-dimensional printers with multiple filaments, Environ. Sci. Technol. 50 (2016) 1260–1268.
[23] M.A. Woodruff, D.W. Hutmacher, The return of a forgotten polymer-polycaprolactone in the 21st century, Prog. Polym. Sci. 35 (2010) 1217–1256.
[24] M. Elbadawi, Rheological and mechanical investigation into the effect of different molecular weight poly(ethylene glycol)s on polycaprolactone-ciprofloxacin filaments, ACS Omega 4 (2019) 5412–5423.
[25] W.Y. Lin, H.Y. Shen, G.H. Xu, L.C. Zhang, J.Z. Fu, X.L. Deng, Single-layer temperature-adjusting transition method to improve the bond strength of 3D-printed PCL/PLA parts, Compos. Pt. A 115 (2018) 22–30.
[26] W.C. Zhang, I. Ullah, L. Shi, Y. Zhang, H. Ou, J.G. Zhou, M.W. Ullah, X.L. Zhang, W.C. Li, Fabrication and characterization of porous polycaprolactone scaffold via extrusion-based cryogenic 3D printing for tissue engineering, Mater. Des. 180 (2019) 107946.
[27] S.H. Teoh, B.T. Goh, J. Lim, Three-dimensional printed polycaprolactone scaffolds for bone regeneration success and future perspective, Tissue Eng. 25 (2019) 931–935.
[28] S. Duan, X. Yang, J. Mao, B. Qi, Q. Cai, H. Shen, F. Yang, X. Deng, S. Wang, Osteocompatibility evaluation of poly(glycine ethyl ester-*co*-alanine ethyl ester) phosphazene with honeycomb-patterned surface topography, J. Biomed. Mater. Res. 101 (2013) 307–317.
[29] W. Liu, S. Liu, Z. Wang, B. Dai, J. Liu, Y. Chen, G. Zeng, Y. He, Y. Liu, R. Liu, Preparation and characterization of reinforced starch-based composites with compatibilizer by simple extrusion, Carbohydr. Polym. 223 (2019) 115122.
[30] M. Esmaeili, G. Pircheraghi, R. Bagheri, V. Altstadt, Poly(lactic acid)/coplasticized thermoplastic starch blend: effect of plasticizer migration on rheological and mechanical properties, Polym. Adv. Technol. 30 (2019) 839–851.
[31] T.K. Dash, V.B. Konkimalla, Poly-epsilon-caprolactone based formulations for drug delivery and tissue engineering: a review, J. Contr. Release 158 (2012) 15–33.
[32] S. Moeini, M.R. Mohammadi, A. Simchi, In-situ solvothermal processing of polycaprolactone/hydroxyapatite nanocomposites with enhanced mechanical and biological performance for bone tissue engineering, Bioact. Mater. 2 (2017) 146–155.